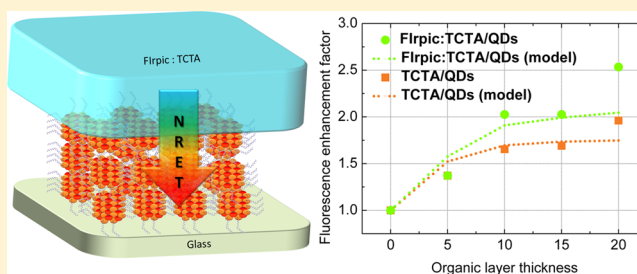


## Singlet and Triplet Exciton Harvesting in the Thin Films of Colloidal Quantum Dots Interfacing Phosphorescent Small Organic Molecules

Burak Guzelturk,<sup>†,‡</sup> Pedro Ludwig Hernandez Martinez,<sup>†,‡</sup> Dewei Zhao,<sup>‡</sup> Xiao Wei Sun,<sup>‡</sup> and Hilmi Volkan Demir<sup>\*,†,‡</sup><sup>†</sup>Department of Electrical and Electronics Engineering, Department of Physics, UNAM – Institute of Materials Science and Nanotechnology, Bilkent University, Ankara 06800, Turkey<sup>‡</sup>Luminous! Center of Excellence for Semiconductor Lighting and Displays, School of Electrical and Electronic Engineering, School of Physical and Materials Sciences, Nanyang Technological University, Singapore 639798, Singapore

## S Supporting Information

**ABSTRACT:** Efficient nonradiative energy transfer is reported in an inorganic/organic thin film that consists of a CdSe/ZnS core/shell colloidal quantum dot (QD) layer interfaced with a phosphorescent small organic molecule (Flrpic) codoped fluorescent host (TCTA) layer. The nonradiative energy transfer in these thin films is revealed to have a cascaded energy transfer nature: first from the fluorescent host TCTA to phosphorescent Flrpic and then to QDs. The nonradiative energy transfer in these films enables very efficient singlet and triplet state harvesting by the QDs with a concomitant fluorescence enhancement factor up to 2.5-fold, while overall nonradiative energy transfer efficiency is as high as 95%. The experimental results are successfully supported by the theoretical energy transfer model developed here, which considers exciton diffusion assisted Förster-type near-field dipole–dipole coupling within the hybrid films.



Phosphorescent small organic molecules have been promising materials for organic light-emitting diodes, owing to their luminescent triplet states, which enabled internal quantum efficiencies up to unity.<sup>1,2</sup> On the other hand, optical properties of the phosphorescent molecules are not versatile; for example, it is difficult to tailor emission color and the full-width at half-maximum (fwhm) of the phosphorescent emission, and the phosphorescence emission is generally wide.<sup>3,4</sup> Alternatively, colloidal quantum dots (QDs) are appealing fluorescent material systems, which are versatile light engines owing to their high photoluminescence quantum yield and ease of color tunability through quantum confinement effect and their narrow emission fwhm.<sup>5,6</sup> Combining the favorable properties of these material systems holds great promise for achieving superior light-emitting materials toward efficient hybrid optoelectronic devices.

Previously, several works reported blended systems of the QDs and the phosphorescent molecules in the form of hybrid thin films.<sup>7–9</sup> In refs 8 and 9, a phosphorescent emitter was shown to enhance the electroluminescence performance of the QDs, which was attributed to the presence of energy transfer from the phosphorescent molecules into the QDs. However, this nonradiative energy transfer in these hybrid thin films was not understood well nor engineered for the singlet and triplet exciton harvesting by the QDs.<sup>10</sup> To date, only Anikeeva et al. have experimentally shown the possibility of nonradiative energy transfer (NRET) in a bilayer thin film of a QD monolayer and green emitting phosphorescent small organic

molecule Irppy<sub>3</sub> codoped CBP. In this architecture, proof-of-concept demonstration of the fluorescence emission enhancement of the QDs was shown by a factor of 1.55.<sup>11</sup> This enhancement was attributed to NRET, which is either due to near-field dipole–dipole coupling or Dexter-type energy transfer. Therefore, the underpinning mechanism of this energy transfer from phosphorescent Irppy<sub>3</sub> molecules, which are doped into CBP fluorescent host, into the QDs was not clear nor understood in this aforementioned work.<sup>11</sup> More importantly, the potential of this type of nonradiative energy transfer in terms of enhancement of the emission of the QDs was not systematically studied before. Also, the effect of fluorescent host (i.e., CBP, TCTA, etc.) to the energy transfer into the QDs in these phosphorescent codoped exciton donor media was not considered. However, these wide bandgap fluorescent host materials are shown here to substantially affect the NRET because excitons are primarily formed in these fluorescent hosts and funneled into the phosphorescent molecules and then transferred into the QDs via NRET.

In this work, we study NRET in a bilayer organic–inorganic thin film consisting of phosphorescent emitter Flrpic that is doped into wide bandgap fluorescent host TCTA, where the organic layer is interfaced to the core/shell CdSe/ZnS QDs. Figure 1a exhibits the representative schematic of the hybrid

Received: September 28, 2014

Revised: October 7, 2014

Published: October 17, 2014

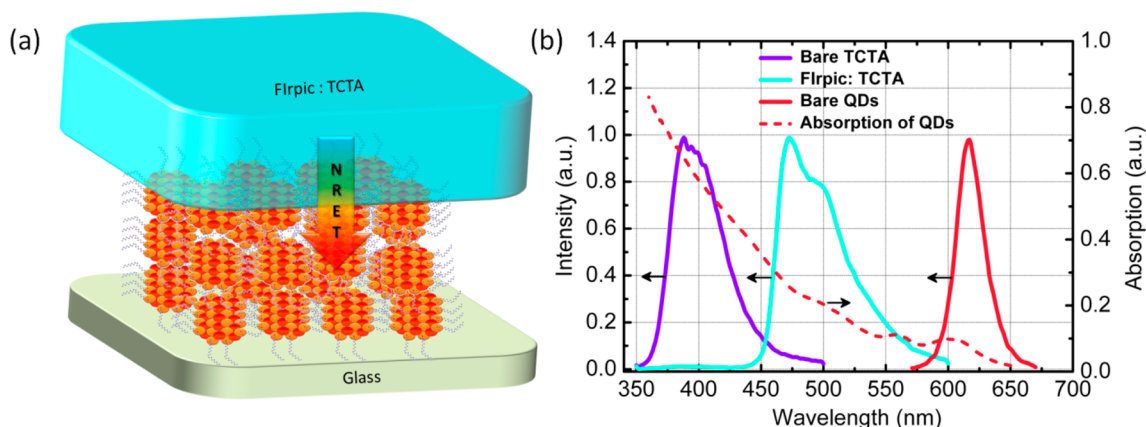


**Figure 1.** (a) Representative schematic of the organic–inorganic exciton transferring thin film. (b) Fluorescence of TCTA (violet), Flrpic (cyan), and QDs (red) along with the absorbance of QDs (red-dashed).

bilayer thin films. Flrpic is a cyan-emitting phosphorescent molecule and is chosen specifically to enhance the spectral overlap between the donor emission and the acceptor QDs' absorption to maximize the critical energy transfer radius (i.e., Förster radius).<sup>12</sup> The acceptor QDs, core/shell CdSe/ZnS, are chosen because of their increased environmental stability and ease of color tunability through the one-pot synthesis route.<sup>13</sup> Additionally, the inorganic ZnS shell thicker than 2 nm helps to block any charge injection into the QDs. We study this energy transfer when TCTA or the Flrpic:TCTA layer is introduced to the QD layer via steady state and time-resolved fluorescence spectroscopies. Also, through photoluminescence excitation (PLE) measurements, we show that NRET actually takes place in the QDs after a cascaded exciton transfer in the organic layer. This type of cascaded energy flow has been observed for the thin films of all organic molecules before, but not for inorganic–organic hybrids.<sup>14,15</sup> When the QDs are interfaced to the phosphorescent codoped organic film, the excitons that were initially funnelled to Flrpic are now transferred to the QDs. Additionally, bare fluorescence host TCTA film is found to be an efficient energy transfer donor for the acceptor QDs even though there is no phosphorescent codoping owing to the efficient singlet exciton harvesting. In the case of Flrpic codoped organic layers, NRET is found to be further enhanced as compared to the case of TCTA alone owing to the increased dipole–dipole coupling and harvesting of the singlet and triplet excitons. To reveal the potential of the NRET in these inorganic–organic systems, we systematically vary the thickness of the organic film from 5 to 20 nm. The maximum enhancement factor of the fluorescence of the QDs is found to be as high as 2.5-fold when the organic film thickness is 20 nm. The theoretical energy transfer model that considers the exciton diffusion assistance to NRET, which is shown to be due to Förster-type dipole–dipole coupling, is proposed. This energy transfer model excellently predicts the experimental fluorescence enhancement factors in the QD emission. In Figure 1b, absorbance and PL spectra of the QDs are shown together with the emission spectra of TCTA and Flrpic. The QDs have broad absorption spectra that match well with the emission of TCTA and Flrpic. Therefore, near-field coupling between Flrpic codoped TCTA film and the QDs is expected to be strong.

The energy transferring thin films are prepared first via spin coating of the QD layer on precleaned glass substrates followed by the thermal evaporation (i.e., sublimation) of the organic

films under high vacuum conditions (base pressure  $<4 \times 10^{-6}$  Torr). The thickness of the QD layer is measured as 20 nm ( $\pm 0.1$  nm) by optical ellipsometry corresponding to an approximately three-monolayer-equivalent QD layer, as also verified by the small root-mean-square surface roughness ( $<2$  nm) via atomic force microscopy. The ellipsometry measurements were performed in the near-infrared region to eliminate the absorption of the red-emitting QDs in the visible. For the organic film, the codoping concentration of Flrpic in TCTA is set as 10% to prevent quenching of the triplet states. The thickness of the organic layer is varied between 5 and 20 nm while keeping the codoping concentration the same. We performed both steady state and time-resolved fluorescence spectroscopy on the film samples including bare QDs, bare TCTA, Flrpic:TCTA, TCTA/QDs, and Flrpic:TCTA/QDs. Figure 2 exhibits the fluorescence of these samples, when excited by a pump wavelength at 330 nm, while the organic layer is 20 nm thick.

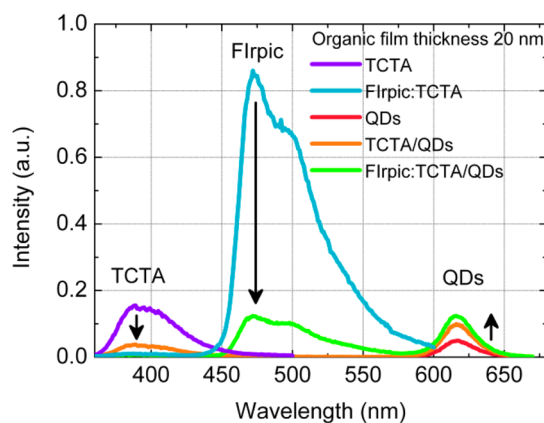


**Figure 2.** Steady state fluorescence spectra of only QDs (red), only TCTA (violet), Flrpic:TCTA (cyan), TCTA/QDs (orange), and Flrpic:TCTA/QDs (green).

As shown by Figure 2, the emission of the TCTA peaks at 388 nm. Flrpic has a peak emission at 470 nm. For the Flrpic:TCTA sample, the emission of TCTA is suppressed considerably due to the almost complete exciton funneling into Flrpic from TCTA.<sup>15</sup> When the organic layer is interfaced with the QDs, the QDs act as an efficient exciton sink for the codoped organic layer. Due to NRET, the emission of TCTA

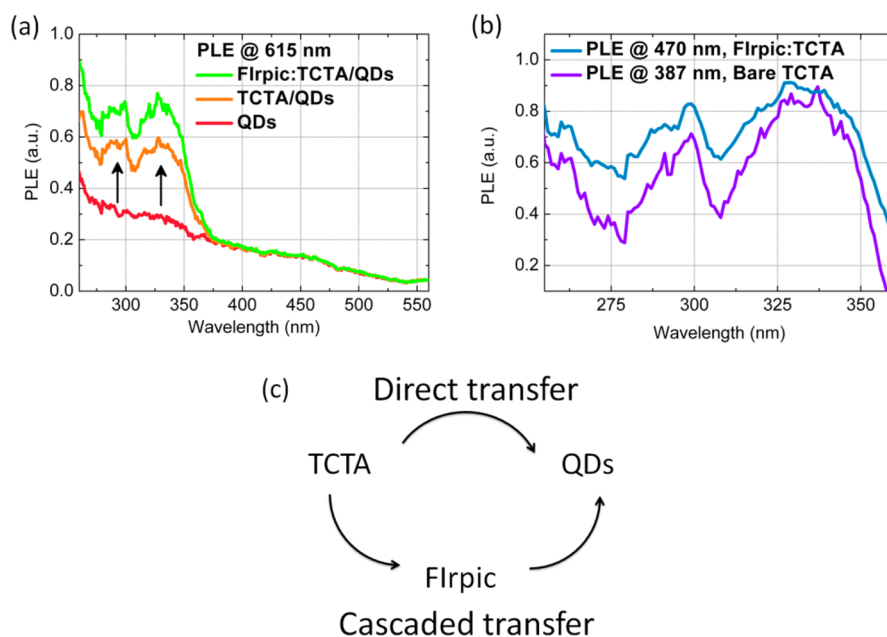


**Figure 3.** (a) PLE at the QD emission peak for the samples of only QDs (red), TCTA/QDs (orange), and Firpic:TCTA/QDs (green) when the organic film thickness is 20 nm. (b) Normalized PLE spectrum of Firpic emission (cyan) from the Firpic:TCTA sample and PLE spectrum of TCTA emission from the bare TCTA sample. (c) Existence of cascaded exciton transfer from the organic layer into the QDs.

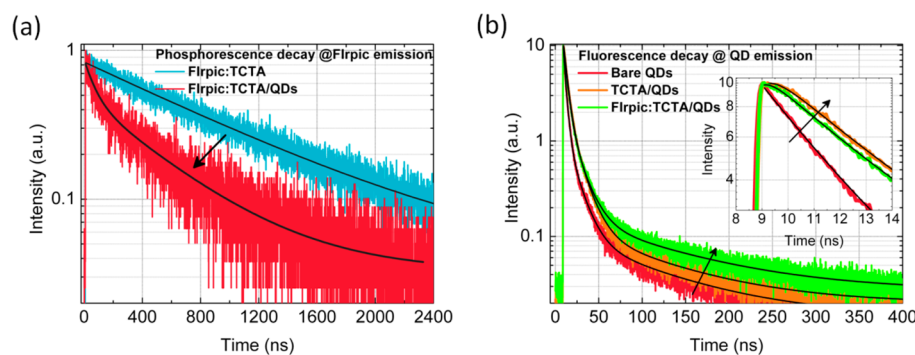


**Figure 4.** (a) Phosphorescence decay curves and their fits for the Firpic emission from the samples of Firpic:TCTA (cyan) and Firpic:TCTA/QDs (red) when the organic film thickness is 20 nm. (b) Fluorescence decay curves and fits for the QD emission from the samples of only QDs (red), TCTA/QDs (orange), and Firpic:TCTA/QDs (green). The inset exhibits the decay in an early time frame. All of the time-resolved measurements were performed using a pulsed laser at 375 nm.

and/or Firpic is quenched, while the emission of the QDs is simultaneously enhanced. Figure 3a shows the PLE spectra measured for the peak emission wavelength of the QDs. For the bare QD sample, the PLE curve (red-solid curve) follows a trend similar to the absorption of the QDs. When the TCTA or Firpic:TCTA energy-transferring organic layer is introduced to the QDs, two additional peaks arise in the PLE spectra of the QD emission around 300 and 330 nm as shown by orange and green curves in Figure 3a. These peaks correspond to the spectral regions where TCTA and Firpic are optically excited as shown by the PLE curves that are measured for the TCTA and Firpic emission peaks in Figure 3b. This enhancement of the PLE of the QDs in these specific spectral regions clearly indicates the transfer of the excitons into the QDs from the organic layer. The PLE enhancement of the QD emission is greater in the case of Firpic:TCTA as compared to the case of the TCTA donor by a factor of 1.25. Since the PLE spectrum of the Firpic emission almost exactly resembles the PLE spectrum at the TCTA emission peak (see Figure 3b), this asserts that Firpic molecules are dominantly excited via strong internal

excitation energy transfer of the excitons in the host materials due to its abundance (90% in our case). This has been observed in the literature for a similar phosphorescent emitter Irppy<sub>3</sub>.<sup>16</sup> Then, these excitons that are primarily generated in TCTA are funnelled to Firpic. As we cannot differentiate the PLE signal of Firpic from that of the TCTA, it is not possible to comment on whether Firpic can actually transfer excitons into the QDs or not from these PLE measurements.

To verify the contribution of Firpic to the NRET, we perform time-resolved fluorescence measurements on these samples using a picosecond pulsed pump laser at 375 nm. Figure 4a depicts the phosphorescent decay curves of Firpic molecules for the Firpic:TCTA and Firpic:TCTA/QDs samples (when the organic film thickness is 20 nm). Firpic phosphorescence decay is significantly accelerated when the QDs are interfaced to the organic layer, which undoubtedly verifies the existence of an exciton transfer channel for the Firpic molecules. Thus, Firpic molecules can clearly contribute to the exciton transfer into the QDs. In the absence of the QDs, the Firpic phosphorescence decay lifetime is 994 ns. When the

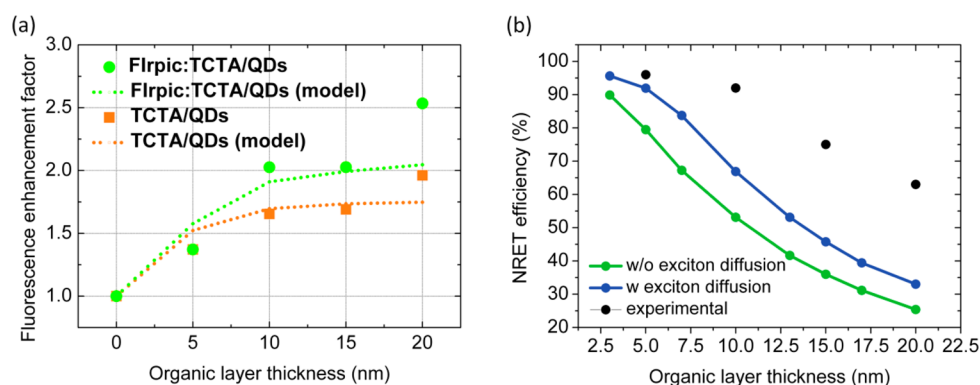


**Figure 5.** (a) Fluorescence enhancement factors of the QD emission in the samples of TCTA/QDs (orange) and FIrpic:TCTA/QDs (green) as a function of the organic film thickness and the modeled enhancement factors plotted in dashed curves. (b) Modeled NRET efficiency in the TCTA:FIrpic/QDs sample as a function of organic layer thickness with and without exciton diffusion assistance together with experimentally measured NRET efficiency from time-resolved fluorescence measurements.

QDs are introduced, the lifetime drops to 366 ns (here a double exponential fit is used with 47.8% of 645 ns and 52.2% of 112 ns). The shortening of the phosphorescence lifetime of FIrpic indicates that a new channel has been opened up for the relaxation of the FIrpic molecules in addition to the intrinsic radiative and nonradiative decay channels. The NRET rate and NRET efficiency are calculated as  $1.72 \times 10^{-3} \text{ ns}^{-1}$  and 63%, respectively. When we investigate thinner codoped organic layers, the lifetime of FIrpic is observed to be much shorter as compared to the thicker codoped layers. This shows that the NRET efficiency grows stronger as the thickness of the organic layer is kept thinner from the donor point of view. In the case of 5 and 10 nm thick codoped organic films interfacing the QDs (QD/FIrpic:TCTA), the FIrpic lifetime is measured to be 40 and 60 ns, respectively. Thus, a surpassing NRET efficiency as high as 95% is achievable in these hybrid QD-phosphorescent doped small molecule based energy transferring thin films. Alternatively, excitons in the hybrid thin films can be transferred directly from TCTA into the QDs as illustrated in Figure 3c in contrast to the cascaded energy transfer route.

In the case of the fluorescence decay of the acceptor QDs, the NRET is independently verified by the observation of slower QD fluorescence decays when the energy-donating TCTA or FIrpic:TCTA is introduced to the QDs as compared to the case of the bare QDs. This slow down of the QD fluorescence decay is attributed to the exciton feeding via NRET. Here, we clarify that the degree of cross-talk between the emission of FIrpic and QDs at the peak emission wavelength of the QDs is negligible (see Supporting Information). The lifetime of the acceptor QDs is increased from 5.07 ns (bare QDs) to 7.87 ns (TCTA/QDs) and 7.80 ns (FIrpic:TCTA/QDs). There is no drastic change in the emission kinetics of the QDs since the time-resolved fluorescence spectra are recorded using a picosecond pump laser at 375 nm, where only a small number of excitons can be generated in the organic layer (see PLE of the TCTA and FIrpic in Figure 3b). Therefore, the QDs are dominantly excited by directly absorbing the pump photons since only a small number of excitons could be nonradiatively transferred from the organic layer. This is also understood by the very little enhancement of the PLE of the QDs at 375 nm as shown in Figure 3a. In Figure 4b inset, the decay of the QDs is shown in the initial time frame, where the decay is slowed down for the samples of TCTA/QDs and FIrpic:TCTA/QDs. This initial

exciton feeding is actually attributed to the fast NRET rate mainly caused by TCTA. Thus, the NRET rate due to TCTA will have a faster rate on the order of  $\text{ns}^{-1}$  as compared to the phosphorescent FIrpic donor, which has a slower NRET rate ( $1.72 \times 10^{-3} \text{ ns}^{-1}$ ) due to the intrinsic slow radiative decay.<sup>17</sup> Therefore, the exciton feeding effects of the phosphorescent molecules to the QDs should be observed over a longer time window as shown in Figure 4b, where the tail of the QD fluorescence decay becomes elongated for the FIrpic:TCTA/QDs sample as compared to the TCTA/QDs and bare QDs samples. This indicates that FIrpic has a slow NRET rate due to the intrinsic slow radiative rate of the phosphorescent molecules.

In Figure 5a experimentally measured fluorescence enhancement of the steady state PL of the QDs as a function of organic film thickness (from 5 to 20 nm in a 5 nm step size) is plotted when the excitation pump wavelength is at 330 nm. The maximum enhancement of the QD emission is 2.5-fold and 2-fold for the FIrpic:TCTA and TCTA donors, respectively. Although NRET efficiency was found to be the highest ( $\sim 95\%$ ) for the thinnest organic layer case (i.e., 5 nm), the fluorescence emission enhancement in the QDs is found to be the highest for the thickest organic layer case (i.e., 20 nm). This phenomenon is attributed to the increased exciton population in the organic film as its thickness is increased, and with the help of exciton diffusion in the codoped organic layer a greater number of excitons can be funnelled into the QDs via NRET as compared to the thinner codoped organic layers. To understand this possible exciton diffusion assistance to the NRET in these bilayer film samples, we devise an NRET model, which combines exciton diffusion in the organic layer in the form of random walk and Förster-type nonradiative energy transfer into the QDs.<sup>18</sup> The exciton diffusion is described as a 3D random walk on a discrete cubic lattice. First, an exciton is optically created in the organic layer with an initial random position within the organic layer while considering the geometric distribution of the excitons in the organic layer due to the absorption profile in the organic layer. Any created exciton can move a single step of length  $\epsilon$  in a random direction after each time interval ( $\Delta t$ ) while being confined to the boundaries of the organic layer unless NRET takes place. The maximum number of steps ( $N_{\text{max}}$ ) required for the exciton to travel a distance equal to the diffusion length  $L_D$  is given by  $N_{\text{max}} = g(L_D/\epsilon)$ , where  $g = 6$  is the degree of freedom. The time step ( $\Delta t$ ) is related to the donor fluorescence lifetime by the

following formula  $N_{\max} \Delta t = \tau_D$ . Then, the NRET rate at each time step is calculated by<sup>19,20</sup>

$$k_{\text{ET}} = \frac{1}{\tau_D} \left( \frac{1}{2} \pi \sigma_{\text{QD}} \right) \frac{R_0^6}{r^4} \quad (1)$$

where  $r$  is the distance between the exciton position and the QD center;  $\sigma_{\text{QD}}$  is the number of QDs per unit area; and  $R_0$  is the Förster radius for the organic layer to the QD pair. The distance dependence is  $r^{-4}$  due to the two-dimensional construct of the acceptor QDs.<sup>20</sup> Next, we define the probabilities for energy transfer during the time step  $\Delta t$  as

$$P_{\text{trans}} = 1 - \exp(-k_{\text{ET}} t) \quad (2)$$

Here  $t = N \Delta t$  is the time;  $N = 0, 1, 2, \dots, N_{\max}$  is the step number; and  $P_{\text{ET}}$  is the probability for an exciton to be transferred to the QD. Substituting eq 1 into eq 2 and using  $t = N \Delta t$  and  $\Delta t = \tau_D / N_{\max}$ , we obtain

$$P_{\text{trans}} = 1 - \exp \left( - \left( \frac{N}{N_{\max}} \right) \left( \frac{1}{2} \pi \sigma_{\text{QD}} \right) \frac{R_0^6}{r^4} \right) \quad (3)$$

To determine whether the exciton is transferred or not, we set  $P_{\text{trans}} > 0.9$ . Thus, if  $P_{\text{trans}} > 0.9$  the exciton is assumed to be transferred, and the random walk of the exciton ends; if not, the exciton diffusion continues to the next time step. This algorithm continues until either the exciton is transferred or the maximum exciton diffusion length is reached.

Now, we estimate the NRET efficiencies as a function of the organic layer thickness. The parameters that are used for the model are diffusion length  $L_D = 15$  nm,<sup>21</sup> random walk step size  $\epsilon = 1$  nm, and QD radius  $R_{\text{QD}} = 3$  nm (as measured by TEM images). At 330 nm, the absorption coefficient of TCTA is about  $3 \times 10^5$  cm<sup>-1</sup>, whereas it is about  $1 \times 10^5$  cm<sup>-1</sup> for the QDs.<sup>22</sup> For the TCTA/QD sample, the Förster radius is estimated to be  $R_0 = 4.957$  nm. For this, the molar extinction coefficient of the QDs is calculated as  $4.1 \times 10^5$  M/cm; the PL quantum yield of the TCTA is used as 20%;<sup>23,24</sup> and the refractive index of the medium is taken as 1.7.<sup>11</sup> The fluorescence lifetime of the TCTA is measured as  $\tau_D = 3.98$  ns. For the TCTA:FIrpic/QD sample, Förster radius is estimated as  $R_0 = 6.030$  nm. The PL quantum yield of the FIrpic is assumed as 80%.<sup>21</sup> The phosphorescence lifetime FIrpic is measured as  $\tau_D = 994$  ns. In Figure 5b, the modeled NRET efficiencies are plotted as a function of organic layer thickness for the case of the TCTA:FIrpic/QD sample. Also, NRET efficiencies are plotted without exciton diffusion assistance to NRET. The exciton diffusion assistance significantly helps for enhanced NRET efficiencies. However, we observe that discrepancy between the exciton diffusion assisted NRET model and the experimental NRET efficiencies increases as the organic layer thickness is increased (see Figure 5b). This indicates that even much stronger exciton diffusion assistance should be active in the energy transfer process of the excitons from the organic phase into the QDs. Then, using the modeled NRET efficiencies and the exciton distribution in the organic layer we calculate the fluorescence enhancement factor of the QD emission. These modeled enhancement factors are plotted as a function of the organic film thickness with dashed lines (see Figure 5a). As can be seen in Figure 5a, the exciton diffusion-assisted exciton transfer model that we propose predicts the photoluminescence enhancement of the QDs with a good agreement until 20 nm organic layer thickness. We

have a slight deviation in the 20 nm organic layer thickness case, and we believe that the discrepancy of organic layer thickness is due to our assumption that exciton diffusion is isotropic in the organic layer. If we were to introduce just a little anisotropy (tendency of diffusion toward the QD layer is slightly larger than the other directions), then we achieve much better agreement (not presented here) in the 20 nm thick organic film. Therefore, exciton diffusion might be anisotropic in these hybrid organic–inorganic films due to an energy gradient toward the interface. These calculated results agree very well with the experimental results.

In conclusion, we studied exciton transfer in a bilayer nanostructure of QDs interfaced with phosphorescent small organic FIrpic molecules in a fluorescent TCTA host via steady state and time-resolved fluorescence spectroscopies. We showed that TCTA alone is an efficient exciton donor for the QDs. On the other hand, utilization of FIrpic increases the exciton funneling into the QDs. Overall, the emission of the QDs is increased up to 2.5-fold. These significant enhancements in the fluorescence of the QDs are found to be due to exciton diffusion assistance to NRET. These findings suggest that such hybrid thin films employing phosphorescent molecules are promising for efficient exciton harvesting.

## ■ ASSOCIATED CONTENT

### ● Supporting Information

Analysis of the cross-talk between the emission of FIrpic and QDs at the peak emission wavelength of the QDs. This material is available free of charge via the Internet at <http://pubs.acs.org>.

## ■ AUTHOR INFORMATION

### Corresponding Author

\*E-mail: [volkan@bilkent.edu.tr](mailto:volkan@bilkent.edu.tr); [hvdemir@ntu.edu.sg](mailto:hvdemir@ntu.edu.sg). Phone: +90 312 290-1021.

### Notes

The authors declare no competing financial interest.

## ■ ACKNOWLEDGMENTS

The authors would like give thanks for the financial support from EU-FP7 Nanophotonics4Energy NoE, and TUBITAK EEEAG 109E002, 109E004, 110E010, 110E217, NRF-RF-2009-09, NRF-CRP-6-2010-02 and A\*STAR of Singapore. H.V.D. acknowledges support from ESF-EURYI and TUBA-GEBIP.

## ■ REFERENCES

- (1) Baldo, M. A.; O'Brien, D. F.; You, Y.; Shoustikov, A.; Sibley, S.; Thompson, M. E.; Forrest, S. R. Highly Efficient Phosphorescent Emission from Organic Electroluminescent Devices. *Nature* **1998**, *395*, 151–154.
- (2) Adachi, C.; Baldo, M. A.; Thompson, M. E.; Forrest, S. R. Nearly 100% Internal Phosphorescence Efficiency in an Organic Light-Emitting Device. *J. Appl. Phys.* **2001**, *90*, 5048.
- (3) D'Andrade, B. Lighting: White Phosphorescent LEDs Offer Efficient Answer. *Nat. Photonics* **2007**, *1*, 33–34.
- (4) Reineke, S.; Lindner, F.; Schwartz, G.; Seidler, N.; Walzer, K.; Lüssem, B.; Leo, K. White Organic Light-Emitting Diodes with Fluorescent Tube Efficiency. *Nature* **2009**, *459*, 234–238.
- (5) Murray, C. B.; Norris, D. J.; Bawendi, M. G. Synthesis and Characterization of Nearly Monodisperse CdE (E = Sulfur, Selenium, Tellurium) Semiconductor Nanocrystallites. *J. Am. Chem. Soc.* **1993**, *115*, 8706–8715.

(6) Demir, H. V.; Nizamoglu, S.; Erdem, T.; Mutlugun, E.; Gaponik, N.; Eychmüller, A. Quantum Dot Integrated LEDs Using Photonic and Excitonic Color Conversion. *Nano Today* **2011**, *6*, 632–647.

(7) Cheng, G.; Mazzeo, M.; Rizzo, A.; Li, Y.; Duan, Y.; Gigli, G. White Light-Emitting Devices Based on the Combined Emission from Red CdSe/ZnS Quantum Dots, Green Phosphorescent, and Blue Fluorescent Organic Molecules. *Appl. Phys. Lett.* **2009**, *94*, 243506.

(8) Zhang, Y. Q.; Cao, X. A. Electroluminescence of Green CdSe/ZnS Quantum Dots Enhanced by Harvesting Excitons from Phosphorescent Molecules. *Appl. Phys. Lett.* **2010**, *97*, 253115.

(9) Cheng, G.; Lu, W.; Chen, Y.; Che, C.-M. Hybrid Light-Emitting Devices Based on Phosphorescent platinum(II) Complex Sensitized CdSe/ZnS Quantum Dots. *Opt. Lett.* **2012**, *37*, 1109–1111.

(10) Guzelturk, B.; Martinez, P. L. H.; Zhang, Q.; Xiong, Q.; Sun, H.; Sun, X. W.; Govorov, A. O.; Demir, H. V. Excitonics of Semiconductor Quantum Dots and Wires for Lighting and Displays. *Laser Photon. Rev.* **2014**, *8*, 73–93.

(11) Anikeeva, P. O.; Madigan, C. F.; Coe-Sullivan, S. A.; Steckel, J. S.; Bawendi, M. G.; Bulović, V. Photoluminescence of CdSe/ZnS Core/shell Quantum Dots Enhanced by Energy Transfer from a Phosphorescent Donor. *Chem. Phys. Lett.* **2006**, *424*, 120–125.

(12) Förster, T. Zwischenmolekulare Energiewanderung Und Fluoreszenz. *Ann. Phys.* **1948**, *437*, 55–75.

(13) Lim, J.; Bae, W. K.; Kwak, J.; Lee, S.; Lee, C.; Char, K. Perspective on Synthesis, Device Structures, and Printing Processes for Quantum Dot Displays. *Opt. Mater. Express* **2012**, *2*, 594.

(14) Baldo, M.; Thompson, M.; Forrest, S. High-Efficiency Fluorescent Organic Light-Emitting Devices Using a Phosphorescent Sensitizer. *Nature* **2000**, *403*, 750–753.

(15) Adachi, C.; Kwong, R. C.; Djurovich, P.; Adamovich, V.; Baldo, M. A.; Thompson, M. E.; Forrest, S. R. Endothermic Energy Transfer: A Mechanism for Generating Very Efficient High-Energy Phosphorescent Emission in Organic Materials. *Appl. Phys. Lett.* **2001**, *79*, 2082.

(16) Tsuboi, T.; Murayama, H.; Penzkofer, A. Energy Transfer in a Thin Film of TPD Fluorescent Molecules Doped with PtOEP and Ir(ppy)<sub>3</sub> Phosphorescent Molecules. *Appl. Phys. B: Laser Opt.* **2005**, *81*, 93–99.

(17) Yuan, X.; Zhao, J.; Jing, P.; Zhang, W.; Li, H.; Zhang, L.; Zhong, X.; Masumoto, Y. Size- and Composition-Dependent Energy Transfer from Charge Transporting Materials to ZnCuInS Quantum Dots. *J. Phys. Chem. C* **2012**, *116*, 11973–11979.

(18) Wu, C.; Zheng, Y.; Szymanski, C.; McNeill, J. Energy Transfer in a Nanoscale Multichromophoric System: Fluorescent Dye-Doped Conjugated Polymer Nanoparticles. *J. Phys. Chem. C* **2008**, *112*, 1772–1781.

(19) Kim, D.; Okahara, S.; Nakayama, M.; Shim, Y. Experimental Verification of Förster Energy Transfer between Semiconductor Quantum Dots. *Phys. Rev. B* **2008**, *78*, 153301.

(20) Hernández-Martínez, P. L.; Govorov, A. O.; Demir, H. V. Förster-Type Nonradiative Energy Transfer for Assemblies of Arrayed Nanostructures: Confinement Dimension vs Stacking Dimension. *J. Phys. Chem. C* **2014**, *118*, 4951–4958.

(21) Lunt, R. R.; Giebink, N. C.; Belak, A. A.; Benziger, J. B.; Forrest, S. R. Exciton Diffusion Lengths of Organic Semiconductor Thin Films Measured by Spectrally Resolved Photoluminescence Quenching. *J. Appl. Phys.* **2009**, *105*, 053711.

(22) Giebink, N. C.; Sun, Y.; Forrest, S. R. Transient Analysis of Triplet Exciton Dynamics in Amorphous Organic Semiconductor Thin Films. *Org. Electron.* **2006**, *7*, 375–386.

(23) Kawamura, Y.; Goushi, K.; Brooks, J.; Brown, J. J.; Sasabe, H.; Adachi, C. 100% Phosphorescence Quantum Efficiency of Ir(III) Complexes in Organic Semiconductor Films. *Appl. Phys. Lett.* **2005**, *86*, 071104.

(24) Jing, P.; Yuan, X.; Ji, W.; Ikezawa, M.; Liu, X.; Zhang, L.; Zhao, J.; Masumoto, Y. Efficient Energy Transfer from Hole Transporting Materials to CdSe-Core CdS/ZnCdS/ZnS-Multishell Quantum Dots in Type II Aligned Blend Films. *Appl. Phys. Lett.* **2011**, *99*, 093106.